Stormy Wave Analysis Based on Recorded Field Data on South-East Coasts of Queensland, Australia

Journal of Coastal Research	SI 64	527 - 533	ICS2011 (Proceedings)	Poland	ISSN 0749-0208

Stormy Wave Analysis Based on Recorded Field Data on South-East Coasts of Queensland, Australia

A. Jafari†, N. Cartwright† and P. Nielsen‡

†Griffith School of Engineering, Gold Coast Campus, Griffith University Southport QLD 4215 Australia, a.jafari@griffith.edu.au n.cartwright@griffith.edu.au

‡ School of Civil Engineering, The University of Queensland Brisbane St Lucia, QLD 4072 Australia, p.nielsen@uq.edu.au

ABSTRACT

A. Jafari†, N. Cartwright† and P. Nielsen, 2011. Stormy wave analysis based on recorded field data on south-east coasts of Queensland, Australia. Journal of Coastal Research, SI 64 (Proceedings of the 11th International Coastal Symposium), 527 – 533. Szczecin, Poland, ISSN 0749-0208

Global warming has lead to a likely increase in the potential of cyclones and storm wind impacts on coastal zones. The behaviour of storm waves in the nearshore is thus one of the most important factors in carrying out risk management and mitigation processes. This paper focuses on the analysis of storm wave data collected in across surfzone during by Cyclone Hamish in 2009. The data was collected by means of a manometer tube system and were analyzed by two different method namely wave-by-wave time domain approach and frequency domain approach. The data is then used to evaluate existing empirical surfzone wave transformation formulae and provides a reliable base for developing more detailed storm wave transformation models.

ADDITIONAL INDEX WORDS: *Tropical cyclones, Monometer Tubes, Wave Setup, Empirical wave parameter, Field study, storm waves*

INTRODUCTION

Understanding of storm wave behavior is critical to the development of appropriate coastal hydrodynamic models to assess risk management and mitigation strategies in response to problems such as coastal inundation and erosion. This is becoming increasingly important in the present age of accelerated global warming where it is expected that there will be an increase in the intensity of severe weather events such as tropical cyclones. One of the main problems associated with the prediction of storm waves, is the lack of availability of field data for calibrating and verifying models. Most of the existing models have been validated based on laboratory data and as such are not entirely representative of storm wave conditions experienced in the field.

So far numerous investigators have tried to extract empirical relationships from recorded data which form the basis of many different wave transformation models (eg., (Nairn, 1990; Raubenheimer et al., 1996; Sallenger and Holman, 1985; Thornton and Guza, 1983; Vincent, 1985)). One of the most well-known parameters is the ratio of wave height to water depth which represented as γ. However, most of the field data analyzed has been obtained in mild to moderate wave conditions. For example, (Thornton and Guza, 1983), measured wave heights at Torrey Beach, California, where the beach profile is low sloped and approximately planar. The wave heights and the average peak frequency of the spectra varied between 0.6m to 1.6m and in the vicinity of 0.07 Hz respectively. The γ values obtained were about 0.6. Further work by (Sallenger and Holman, 1985) found that γ_s is dependent on the beach slope which values ranged from about 0.4 to 0.8, but independent of the offshore wave steepness. These data were collected during storm, $1.96 < H_o < 2.4$; $6.9 < T_p < 16.8$ at Duck, North Carolina. However, (Nairn, 1990) suggested that γ_s increases with increasing offshore wave steepness. He combined low and high wave steepness data collected on barred and unbarred beaches in the laboratory and field. The data used by (Nairn, 1990) were collected during hurricane Eloise on the Florida coast. H_{rms} and peak period vary between 1m to 2.6m and 6s to 14s respectively.

To the knowledge of the authors, the only known field data set collected during storm conditions are those of (Vincent, 1985) in which significant wave height reaches 5m in 36m depth buoy. Based on his observations he suggests that the significant wave height was proportional to $h^{1/2}$ ($\gamma_s \propto h^{-1/2}$) in the outer surf zone but γ_s was approximately constant in the inner surf zone. However, (Vincent, 1985) did not proposed specific formulation purely for storm condition in his work.

METHODOLOGY

This paper presents the analysis of field data collected under storm conditions. The data was collected at a field site at the Spit on the Gold Coast, Australia. Situated in south-east Queensland, the Gold Coast has a sub-tropical climate in which storm wave conditions normally occur during the summer months due to cyclones and east coast lows.

Equipment and Infrastructure

In order to obtain coastal water level and wave measurements, permanent infrastructure was installed at the Spit on the Gold Coast, Queensland. The Facility utilises an array of permanently deployed manometer tubes to observe both time-averaged (mean) water levels (MWL) and high-frequency pressure fluctuations due to wave action at 12 locations through the surfzone (Figure 1).

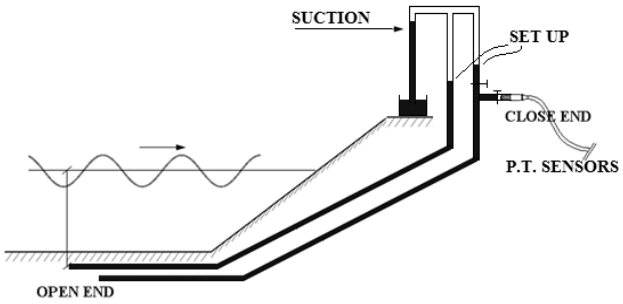

: Sketch of manometer tube array, exerting suction make 1Figure it possible for reading

The manometer tube system is a simple but very robust means of measuring and monitoring wave trains while they travel from 500m offshore through the inner surfzone. It also provides the opportunity to observe the mean water level and high frequency water level fluctuations (waves) simultaneously. The land based monitoring station and permanent deployment of the tube array enable the safe collection of storm surge and storm wave data during severe events. The application of the manometer tube system in this way was first developed by (Nielsen, 1986). Theoretical details of the system can be found in (Nielsen and Dunn, 1998) and a description of Gold Coast facility can be found in (Cartwright et al., 2009)

As the water level setup profile tends to become steeper between the inner surf zone and the swash zone, the data collected using the manometer tubes is supplemented with temporarily installed stilling wells across the very near shore and swash zone in order to more accurately track the mean shoreline position with higher resolution (Figure 2).

In addition, self logging pressure sensors are also used to record the wave and water pressure in inner surf zone. The maximum water depth that these types of sensors deployed is about 2 meter depth which means that the water is shallow enough so the recorded pressure represents the exact water depth and wave height. Therefore, there is no point of having concern about the effects of water particle movement on dynamic pressure which have been recorded by sensors. The data from this type of sensors also helped us to double check the results of manometer tube system for the same span that they both have covered it. Normally self logging pressure transducers have been set up along with stilling wells which can be seen in Figure 3.

. Stilling Well shows the long wave water level fluctuation 2Figure

. Stilling Well (right) and Self Logging Pressure 3Figure Transducer (left) deploying across the swash Zone in Low Tide; Cyclone Hamish May 2009

Field Data Collection

Generally, the mean water surface level in the ocean is below the ground level at the land based monitoring station and so suction is applied in order to draw the water levels above ground. This is done in an enclosed system with each tube being subjected to the same degree of suction thus preserving the relative water differences between each tube. The absolute level of all tubes is then converted to the Australian Height Datum (AHD) by including a surveyed static water level into the manometer board system so that it also experiences the applied suction. The water level in water reservoir is exposed to atmospheric pressure, thus the column of water which climbed inside the reference board shows the amount of suction inside manometer system (Figure 1).

High frequency water level fluctuations due to wind waves are recorded by connecting pressure transducers directly to the landward end of the tube system (Figure 1). The raw voltage output from each of the sensors is logged at 10 Hz using a data acquisition card connected to a laptop computer. The raw voltage data is then converted to a pressure head by means of a calibration equation derived from laboratory tests. However, the manometer tube systems behaves as a resonating system with one end of the tube open to the wave fluctuations and the other blocked by a pressure transducer. In order to correct for resonance effects, a gain function is applied to convert the pressure observed at the landward end of the tube to a seabed pressure at the seaward end of the tube. (Nielsen and Dunn, 1998) performed laboratory tests to establish the following empirical gain function for a similar tube system,

$$G = \frac{1}{\sqrt{\left(\cos^2\left(\frac{\pi \times f}{2 f_o}\right) + \left[B_1 \frac{L \times f}{c}\left(1 + B_2\sqrt{\frac{\nu}{f \times d^2}}\right)\right]^2\right)}} \quad (1)$$

where, ν is fluid viscosity (for water $\nu = 1.0\times10^{-6}\ m^2/s$), f_0 is the lowest resonance frequency, i.e., $L = 0.25\times c/f_0$, B_1=0.58 and B_2=5.0. c, is speed of waves sound in flexible tubes which can define as

$$c = \frac{1}{\sqrt{\rho(K + D)}} \quad (2)$$

where, K is the compressibility of the fluid and D is the distensibility of the tube. Although the form of equation (1) is based on theoretical considerations, it must be expected that the constants, B_1 and B_2, may vary somewhat with tube material and dimensions. Note that the second term in equation (1), represent the Energy loss in term of heat of fluid due to viscosity (Nielsen et al., 1993). The agreement between equation (1) and the calibration data is shown in Figure 4

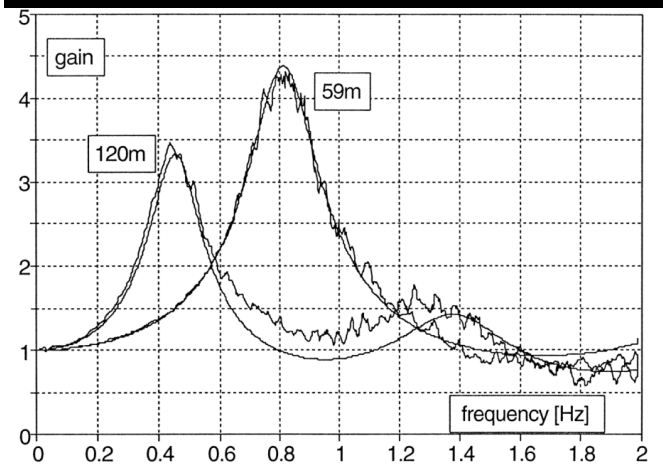

. Gain function for 120m and 59m tube length after 4Figure (Nielsen and Dunn, 1998)

Upgrading Experimental Factor

In order to improve the accuracy of the Gain Function, extensive laboratory test were conducted to deteremine the value of the two dimenssionless empirical factors, B1 and B2., for tube lengths ranging from 10m to 900m whose properties are shown in Table 1.

In this test, the tubes were filled with water and one end of the tube was oscillated in a sinusoidal fashion by modifying an electro motor. The pressure at both ends of the tube were recorded simultaneously and the gain subsequently calculated. The GF for each period was independently calculated by two method, namely time domain zero up crossing and Spectral method. As shown in Figure 6, both method, return same value with 2 decimal accuracy. Utilizing the electro motor, give us an opportunity to just make a constant frequency of ocsilation in each duration of recording. The advantage of this method, rather than manually create a range of frequencies, is to eliminate superposition of different frequencies in extracting the GF which affects the amount of peak as well as peak frequency.
By applying new dimensionless factor, B_1 and B_2, and replot the GF, result showe very good agreement with Laboratory data. By curve fitting (see Figure 5) following relations can be extract from B_1 and B_2 in term of length over outer diameter ratio of tubes:

$$B_1 = \pi \times \left(L/OD\right)^{\frac{t}{ID}} \quad (3)$$

$$B_2 = \left(2 \times OD/t\right) \times e^{-6\times10^{-6}\times(L/OD)} \quad (4)$$

where, L is tube length, OD is tube outer diameter, ID is tube inner diameter, t is tube thickness. Therefore equation (1) can be calculated for any length of tube independent of empirical factors.

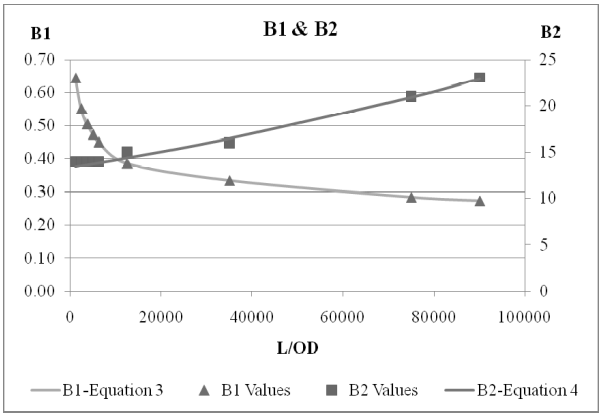

(4) and (3). B_1 and B_2 Values agains Equations 5Figure respectively

Extracting Wave Height out of Seabed Pressure

The next step in the data processing is to convert the seabed pressure to a free surface elevation by correcting for the dynamic pressure distribution under wave motion. This is achieved via the local approximations approach of (Nielsen, 1989) which is based on the assumption that all surface waves are harmonic and can be define by a combination of suitable harmonic functions.

Table 1. Tube properties tested in Lab

Tube Length (m)	OD (m)	ID (m)	t (m)	New B_1	New B_2
10	0.008	0.0054	0.0012	0.64	13.7
20	0.008	0.0054	0.0012	0.55	13.8
30	0.008	0.0054	0.0012	0.50	13.9
40	0.008	0.0054	0.0012	0.47	14.0
50	0.008	0.0054	0.0012	0.45	14.1
100	0.008	0.0054	0.0012	0.39	14.7
350	0.01	0.007	0.0015	0.33	16.8
750	0.01	0.007	0.0015	0.28	21.4
900	0.01	0.007	0.0015	0.27	23.4

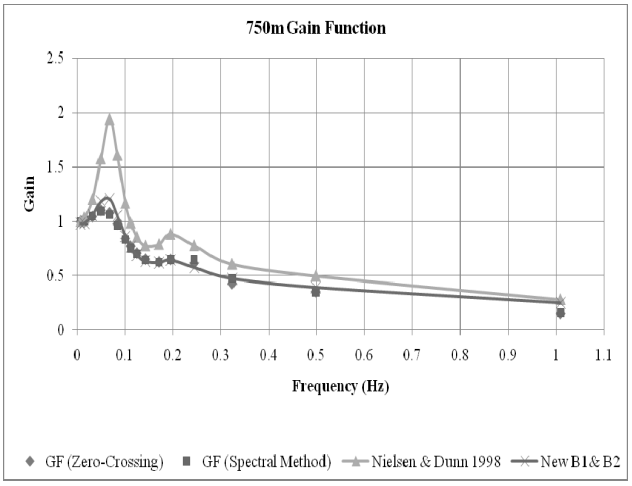

Figure 6. Gain Function for 750m tube, equation (1) against laboratory data, and also fitted GF with new B1 & B2 fited

For an irregular wave in the ocean, a local frequency for the water level fluctuations for each point in time can be defined. For example, for a sinusoidal shape like $y(t) = A_n \sin(\omega_n - \varphi_n)$, the three adjacent data points y_{n-1}, y_n , and y_{n+1} can be used to approximate the local angular frequency for the nth point by,

$$\omega_n^2 = \frac{-y_{n-1} + 2y_n - y_{n+1}}{\delta^2 y_n} \tag{5}$$

where δ is sampling time interval.

For the conversion of seabed pressure to a free surface elevation, (Nielsen, 1989) introduces the following semi-empirical function,

$$\hat{\eta}_n = \frac{p_n}{\rho g}\exp\left[A\left(\frac{z}{h}\right)\frac{-p_{n-M} + 2p_n - P_{n+M}}{g(M\delta)^2 p_n}\left(h + \frac{p_n}{\rho g} - z\right)\right] \tag{6}$$

with A being an experimental factor related to the depth of recording the dynamic pressure (p)

$$A\left(\frac{z}{h}\right) = 0.67 + \frac{0.34z}{h} \tag{7}$$

where, h is water depth and z is depth of installing device for recording dynamic pressure. M is a numerical parameter used for smoothing the curvature of water elevation. Instead of just picking first neighbors of n^{th} point to for estimation of water elevation, here the M^{th} neighbors have been picked.

Once the free surface time series has been established the wave statistics (height, period etc) are derived using the usual spectral analysis and zero-crossing approaches.

DATA VERIFICATION AND ANALYSIS

The recorded data is verified against data from a nearby wave rider buoy and tide gauge. For example, Figure 7 shows the comparison between the mean water level recorded by the monometer tubes and the Maritime Safety tide gauge data. Figure 7 shows the good agreement between what has been recorded by different tube lengths in manometer tube system and that from a nearby tide gauge.

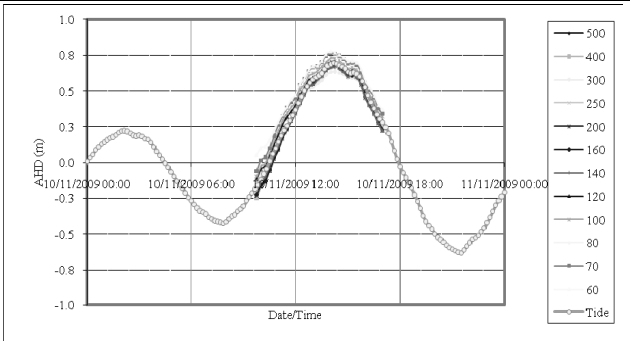

. Recorded water level for each tube and verified it 7Figure by Maritime Safety Gauge data

RESULT AND DISCUSSION

One of the most important data which needs to be collected is beach profile bathymetry. As it is almost impossible to do the surfzone bathymetry profile surveying during severe storms, it is better to do it regularly every one or two months to have the most updated beach profile before for each upcoming storm. Figure 8 shows the recorded bathymetry of our field site before and after TC Hamish. By combining the beach profile data with the recorded mean water level data from monometer tube system, the water depth for seaward end of each tube can be determined.

Consistent with data obtained from the nearby Gold Cost wave rider buoy, the manometer tube wave data was divided into thirty minute time blocks and wave characteristics were extracted using both spectral and zero-crossing approaches. The energy density and time series of water fluctuation for 250m tube is represented in Figure 9 and Figure 10 respectively as well as the wave corresponding wave height for each graph.

Both approaches generally show good agreement with the buoy data. Considering the depth and offshore distance where wave rider buoy is located (1200m offshore and 18m depth) and also the fact that the waves are subjected to transformation process (e.g. refraction, shoaling) while they travel between the buoy and the

tubes, it is expected that some differences between the tube and buoy data sets will exist. The comparison between the Gold Coast Buoy and tube system for different time-block data is shown in Table 2. Significant wave height (H_s) and maximum wave height (H_{max}) are derived from the zero-crossing method.

The average wave height and average wave period obtained from zero-crossing method along the surf zone for each tube are illustrated in Figure 11. As it can be interpreted from Figure 11 first breaker line is somewhere between 250m and 200m offshore, and the second breaker line is somewhere between 160m and 140m.

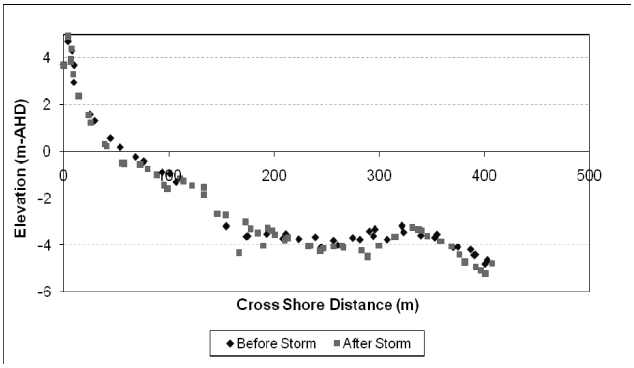

. The recorded bathymetry of our field site before and 8Figure after TC Hamish

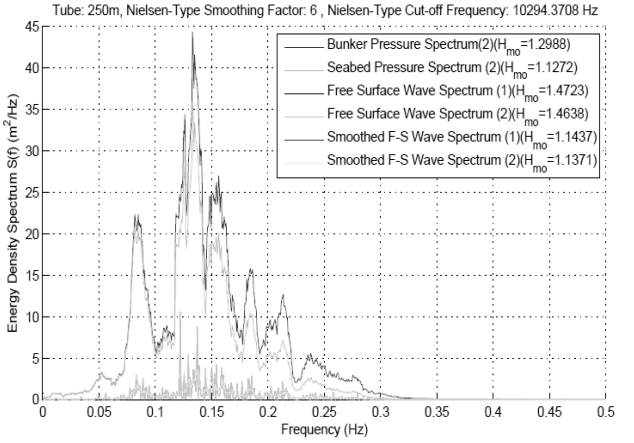

Figure 9. Energy Density Spectrum of the data recorded by 250m tube

Current expressions about the behavior of γ_s, the ratio of significant wave height over water depth, have been examined by recorded data. As it illustrated in Figure 12, (Thornton and Guza, 1983) and also (Sallenger and Holman, 1985), don't show good agreement with the recorded data. Moreover, (Nairn, 1990) expression doesn't agree with the data at all. The only expression that in some extent can represent the pattern of changing the γ_s, is (Vincent, 1985) which highly required to be modified since the γ_s values haven't shown constant values in inner surf zone. In addition in outer surf zone, it isn't delicate enough to mention that

$\gamma_s \propto h^{-1/2}$. Actually it is necessary to consider the breaking points as a factor to dissipate the wave energy which influences both wave height and γ_s. Sudden drop of wave height at breaking points can be induced that the pattern of γ_s changing is different between each breaker lines. Figure 13, represent the different pattern of γ_s when the recorded data have been divided into three different zone, first zone is before first break, second zone is after first break and before second break, and the third zone is inner surfzone which is after second break.

By this zoning, obviously the linear changing pattern of γ_s can be taken out which is so helpful in extracting the dissipation model of wave energy rather than taking nonlinear relation of γ_s into account. As it can be seen in Figure 13, in all three mentioned zone, γ_s change with negative slope according to the related depth; however, while wave approach to the beach from offshore, the depth is decreasing so on the other hand if you travel with the wave, γ_s, tend to increase. Then after reaching each breaking point regarding to the related depth, it has a sudden drop.

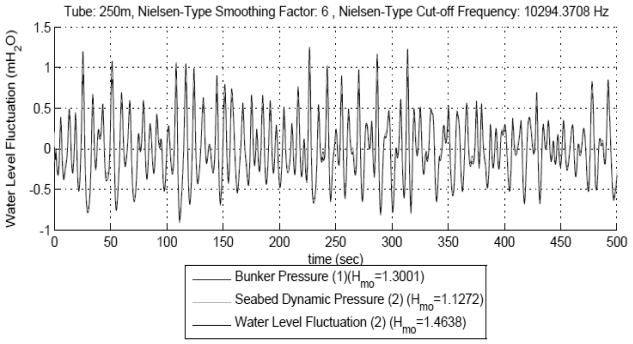

. Time series of water surface fluctuation of the data 10Figure recorded by 250m Tube for first 500 second

Table 2. Wave characteristics of Gold Coast Buoy (GCB) against Manometer Tube System

Tube Length / Time-Block	H_{sign} (Zero-up)					H_{max} (Zero-up)				
	400	**300**	**250**	**200**	**GCB**	**400**	**300**	**250**	**200**	**GCB**
9:00:00 AM	2.37	1.91	1.96	2.15	2.11	3.6	2.58	2.93	3.24	3.6
9:30:00 AM	2.39	1.91	2.06	2.16	2.18	3.43	2.47	2.79	3.17	3.32
10:00:00 AM	2.67	2.11	1.98	2.15	2.22	3.91	2.76	2.95	3.15	4
10:30:00 AM	2.81	2.01	1.96	2.18	2.19	3.66	2.97	3.47	2.94	3.12
11:00:00 AM	2.54	2.04	1.98	2.39	2.03	3.82	2.78	3.16	6.75	3.54
11:30:00 AM	2.68	1.93	1.93	2.16	2.15	3.43	2.84	2.81	3.21	3.48
12:00:00 PM	2.65	1.88	1.81	2.06	2.16	3.42	4.58	2.64	3.53	3.54

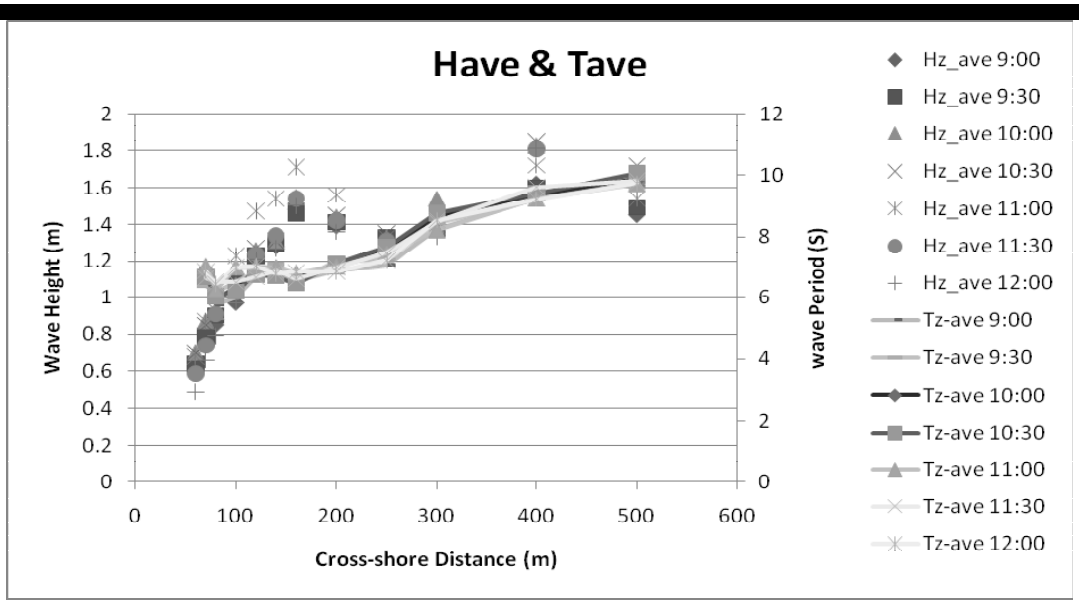

. Average wave height and average wave period of different 30min block11Figure

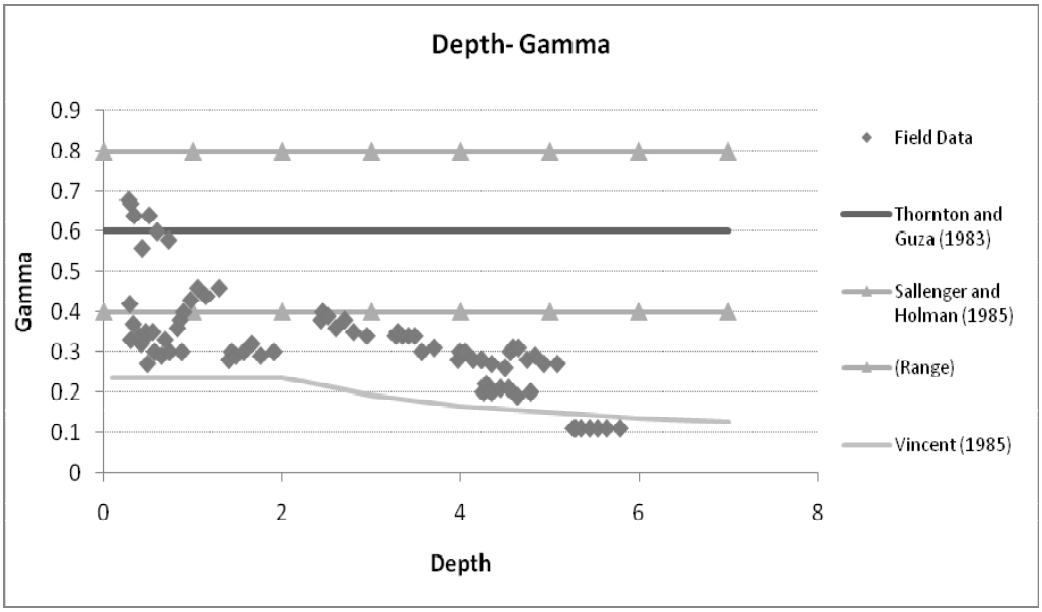

. Current Expresion about γ_s agains recorded field data12Figure

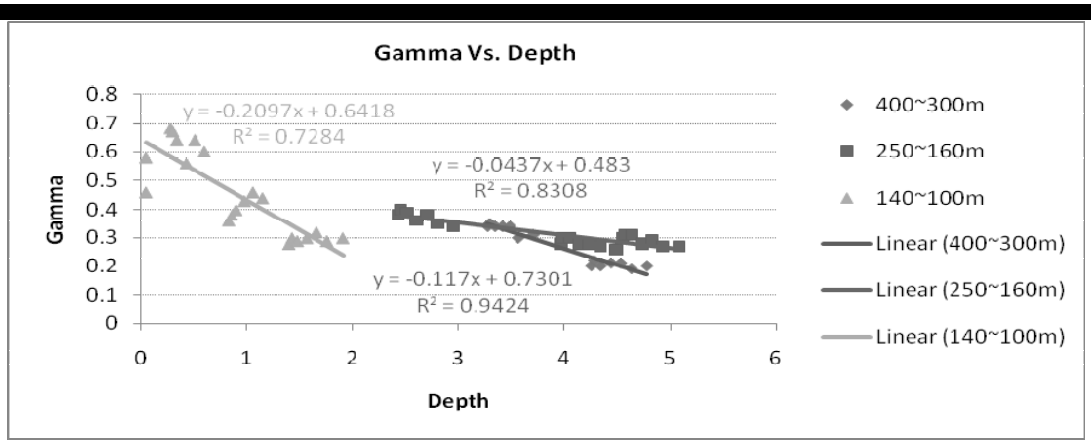

. Changing pattern of γ_s Extracted from recorded field data13Figure

CONCLUSION

The result of this paper indicates that, the existing expressions for the experimental wave height to water depth ratio, γ_s, don't reflect exactly what happened while storm wave trains travel from offshore toward inner surf zone. In order to develop and accurate model of energy dissipation based on actual field data, it is essential to represent γ_s as simple as possible. By considering the 3 zones: offshore, beyond first breaking point, between two breaking points, and landward of the second breaking point, the relationships between γ_s and depth are essentially linear. As presented in Figure 13, the slope of γ_s vs h are different in each zone which reflects the portion of different dissipation factors (i.e. friction, slope, and breaking intensity). In addition, when γ_s reaches 0.4 for, the breaking happens which means that this surfzone known as unsatuarated. Furthermore, 25% and 30% reduction take place in γ_s after each break point for first zone and second zone respectively. These boundary conditions are going to be used in developing a wave transformation model base on recorded field data under storm conditions.

REFERENCES

Cartwright, N., Callaghan, D.P. and Nielsen, P., (2009). Coastal Field Research Facility: The Spit, Gold Coast, Australia, The University of Queensland.

Nairn, R.B., (1990). Prediction of cross-shore sediment transport and beach profile evolution, University of London, London, England.

Nielsen, P., (1986). Local approximations: A new way of dealing with irregular waves. Proc. 20th Int. Conf. Coastal Engineering. Taipei, Taiwan: 633-646.

Nielsen, P., (1989). Analysis of Natural Waves by Local Approximations. Journal of Waterway, Port, Coastal, and Ocean Engineering, 115(3): 384-396.

Nielsen, P. and Dunn, S.L., (1998). Manometer tubes for coastal hydrodynamics investigations. Coastal Engineering, 35: 73-84.

Nielsen, P., Hanslow, D.J. and Apelt, C.J., (1993). A new type of nearshore wave gauge. 11th Aust. Conf. Coastal Ocean Eng. Townsville.: 247-251.

Raubenheimer, B., Guza, R.T. and Elgar, S., (1996). Wave transformation across the inner surf zone. Journal of geophysical research, 101: 25,589-25,597.

Sallenger, A.H. and Holman, R.A., (1985). Wave energy saturation on a natural beach of variable slope. Journal of geophysical research: 11,939-11,944.

Thornton, E.B. and Guza, R.T., (1983). Transformation of Wave Height Distribution. Journal of geophysical research, 88: 5925-5938.

Vincent, C.L., (1985). Depth-controlled wave height. Journal of Waterway, Port, Coastal and Ocean Engineering, iii: 459-475.